Biosensors and Bioelectronics 223 (2023) 115008

Contents lists available at ScienceDirect

Biosensors and Bioelectronics

journal homepage: www.elsevier.com/locate/bios

New trends in methyl salicylate sensing and their implications in agriculture

A.M. Ashrafi [a,b,1], Z. Bytešníková [a,1], C. Cané [c], L. Richtera [a,b], S. Vallejos [b,c,*]

[a] Department of Chemistry and Biochemistry, Mendel University in Brno, Zemedelska 1, 613 00, Brno, Czech Republic
[b] CEITEC - Central European Institute of Technology, Brno University of Technology, Purkynova 656/123, 612 00, Brno, Czech Republic
[c] Institute of Microelectronics of Barcelona (IMB-CNM, CSIC), Campus UAB, 08193, Cerdanyola del Vallès, Barcelona, Spain

ARTICLE INFO

Keywords:
Methyl salicylate sensing
Methyl salicylate monitoring
Chemical sensor
Biosensor
Gas sensor
Plant protection

ABSTRACT

Methyl salicylate (MeSal) is an organic compound present in plants during stress events and is therefore a key marker for early plant disease detection. It has usually been detected by conventional methods that require bulky and costly equipment, such as gas chromatography or mass spectrometry. Currently, however, chemical sensors provide an alternative for MeSal monitoring, showing good performance for its determination in the vapour or liquid phase. The most promising concepts used in MeSal determination include sensors based on electrochemical and conductometric principles, although other technologies based on mass-sensitive, microwave, or spectrophotometric principles also show promise. The receptor elements or sensitive materials are shown to be part of the key elements in these sensing technologies. A literature survey identified a significant contribution of bioreceptors, including enzymes, odourant-binding proteins or peptides, as well as receptors based on polymers or inorganic materials in MeSal determination. This work reviews these concepts and materials and discusses their future prospects and limitations for application in plant health monitoring.

1. Introduction

With the growth of the world population, the demand for agricultural production has increased. Simultaneously, global climate changes have favoured plant pathogens, enabling their spread into new regions (Baker et al. 2000). Newly occurring pathogens can overcome plant defences and cause new epidemics (Anderson et al. 2004), putting the global production of food at risk (FAO, 2017). In addition to modern strategies that use nanomaterials against plants pathogens (Bytesnikova et al. 2022), the detection of volatile organic compounds (VOCs) naturally emitted by plants is another intelligent strategy for agriculture in the 21st century to control plant health and avoid spreading diseases (Ivaskovic et al. 2021; Jansen et al. 2011; Li et al. 2019a,b,c,d). The emission of VOCs from different parts of the plant can be induced in response to biotic (Dicke and Baldwin, 2010) or abiotic stresses (Loreto and Schnitzler, 2010). Plants are able to memorize stressful situations that they experience (Crisp et al. 2016; Hilker et al. 2016) and thus can respond to ongoing stressful situations. This stress memory of plants is achieved by so-called priming stimuli, in which VOCs play an important role due to their volatility, which enables them to easily and quickly reach remote parts of their host plant or other plants (Shulaev et al. 1997; Baldwin et al. 2006; Mauch-Mani et al. 2017). Ethylene, terpenoids, methyl jasmonate, and methyl salicylate are examples of VOCs that act as signal communicators (Baldwin et al. 2006; Singewar et al. 2021). Thus, the detection of these single compounds or their mixtures (with each other or with other substances) could provide a step forward in the development of smart systems for plant protection.

Specifically, methyl salicylate (MeSal) is one of the products of salicylic acid (SA) metabolization and serves as a signal molecule in the hormone regulation of plant life activities. Upon infection, MeSal is released rapidly and in large amounts from plants (Huang et al. 2003). For instance, studies on healthy and infected tobacco plants provided evidence of MeSal as a first airborne signal that may activate disease resistance in the healthy tissues of the infected plant and neighbouring plants (Shulaev et al. 1997). This proved that MeSal is a mediator of interplant communication and a very attractive target analyte in agriculture for the early detection of possible infections and prevention of huge crop losses. It is also worth noting that MeSal significance goes beyond agriculture and extends to other sectors, including the food industry (Sharma et al. 2016) (where it is used as a flavour additive),

* Corresponding author. Institute of Microelectronics of Barcelona (IMB-CNM, CSIC), Campus UAB, 08193, Cerdanyola del Vallès, Barcelona, Spain.
E-mail address: stella.vallejos@imb-cnm.csic.es (S. Vallejos).
[1] Both authors contributed equally.

https://doi.org/10.1016/j.bios.2022.115008
Received 30 March 2022; Received in revised form 8 December 2022; Accepted 12 December 2022
Available online 13 December 2022

pharmaceutics (Krzek et al. 2003) (for pain relief) and security (Matar et al. 2016) (as a chemical warfare agent simulant), among others.

Generally, MeSal from plants is determined in the gas or liquid phase extracted either from the plant environment or from the plant itself. MeSal can also accumulate under dense canopies, roofs, or any other type of plant cover, where it can be measured. Currently, the determination of MeSal, at experimental or laboratory levels, is carried out by conventional analytical techniques. For instance, chromatographic separation by either gas chromatography (GC) (Abraham et al. 1976; Cai et al. 2015; Deng et al., 2004a, 2005; Huang et al. 2015; James et al. 2019; Li et al., 2019b; Mazurek and Szostak, 2016; Stevens and Warren, 1964) or high-performance liquid chromatography (HPLC) (Adzib and Ilham, 2020; Parker et al. 2004) can be coupled with detection techniques such as thermal conductivity (Abraham et al. 1976; Stevens and Warren, 1964; Li et al. 2021; Anyakudo et al. 2019; Lau et al. 2018; Magagna et al. 2017), ultraviolet-visible spectroscopy (UV-Vis) (Adzib and Ilham, 2020; Parker et al. 2004; Shabir and Bradshaw, 2011), mass spectrometry (Cai et al. 2015; Deng et al., 2004a; Huang et al. 2015), Raman spectroscopy (Park et al. 2020a,b), or flame ionization detection (FID) (Li et al., 2019b) for MeSal determination. The incorporation of preconcentration steps with these techniques is also a frequent practice to further lower the limits of detection (LODs). Namely, headspace solid-phase microextraction (HS-SPME) (Deng et al., 2004a), ultrasound-microwave synergistic extraction (Li et al., 2019b), and thermal desorption (Cai et al. 2015) were applied for the extraction of MeSal in a preconcentration step. These conventional methods offer sensitive and accurate determination of MeSal; however, their need for sophisticated instrumentation, skilled technicians, and consumables (usually large volumes of organic solvents for the extraction or determination step) may increase their cost and confer environmentally harmful characteristics. Other issues associated with conventional methods also include their poor suitability for direct on-field measurements, and although the new portable GC samplers and detectors may solve this issue in part, their deployment for real-time monitoring still represents drawbacks compared to other miniaturized sensors used in electronic noses (e-nose) (Tholl et al. 2021).

Hence, there is a need for a new generation of VOC sensors with miniaturized, lightweight, low-cost, and high-performing properties that allow not only the *in-situ* monitoring of plant volatiles but also the detection of specific markers of plant defence as MeSal. By applying such sensors, the sampling and sample preparation steps can also be avoided, thus decreasing the analysis time and cost. Current micro/nano-fabricated chemical sensors based on advanced semiconductors (e.g., metal oxide nanowires (Vallejos et al. 2015)), polymers (e.g., polypyrrole (Setka et al. 2020)), carbon-based materials (e.g., graphene oxide (Sedlackova et al. 2020)), organic dyes (e.g., cysteine (Li et al., 2019b)), or bioreceptors (e.g., enzymes) (Ashrafi et al. 2019)) coupled with other elements processed by silicon technology (Vallejos et al. 2016; Chmela et al. 2018) or printed electronics (Conti et al. 2020; Ge et al. 2022) meet these technological, cost, and production needs. Previously it was identified that these sensing technologies could facilitate the practical implementation of sensory networks for plant protection (Li et al., 2019b; Yang, 2020; Fang and Ramasamy, 2015; Garlando et al. 2020; Burgués and Marco, 2020) using new concepts for data processing at the edge and connecting remotely online with other systems in line with the coming *Agriculture 5.0* (Yang, 2020; Saiz-Rubio and Rovira-Más, 2020).

Recent literature reviews also identify the technological needs for agriculture and plant protection by focusing on specific aspects. For instance, the new multisensory systems and mathematical models developed so far for monitoring odour clouds from plants and animals (Ivaskovic et al. 2021), the sampling and analysis of odour clouds containing VOCs from agriculture (Tholl et al. 2021), the nanomaterials for biosensing of plant pathogens (Cardoso et al. 2021), or the most appropriate technologies for deploying unmanned aerial vehicles able to map gaseous source localization and identification (Burgués and Marco, 2020). In addition, a recent review of signalling processes in plants points out the critical role of MeSal in the health of forest ecosystems (Singewar et al. 2021). In this context, the present review contributes further to identifying miniaturized sensing technologies with potential in plant protection, thus, bringing a new and comprehensive view (not discussed previously) of the methods and strategies employed for MeSal as a key volatile signalling marker of plant defence. Table 1 summarizes and compares the scope of this and previous reviews, manifesting the timeliness of this discussion.

Hence, the present review focuses on (bio)chemical sensors, their main characteristics and performance indicators towards MeSal, as well as the current limitations and future prospects of miniaturized sensors for plant health monitoring.

2. MeSal as a participant in plant defence

When pathogens infect a plant, they replicate and spread rapidly throughout the plant body, which may result in the death of the plant and infection of surrounding plants. Studies on the emission of VOCs from plants showed that the amounts of MeSal increase rapidly after infection, usually on the order of tens of ppb or hundreds of $ng{\cdot}L^{-1}$, as determined for infected tobacco (Shulaev et al. 1997) and tomato (Chen et al. 1987; Deng et al. 2004a,b) plants. In some species in forest ecosystems, MeSal concentrations reach a level sufficient for its characteristic aroma to be easily perceivable to the human nose (Singewar et al. 2021). If a resistant plant is infected, a large arsenal of physiological and biochemical responses is induced. These responses protect the plant against pathogens and potential damage. Plant resistance development occurs within several days to a week and is manifested by the limitation of pathogens around the infection site, where tissue necrosis can appear. During this period, resistance against the same or even an unrelated pathogen increases, and this process is known as systemic acquired resistance (SAR).

The occurrence of SAR (Fig. 1) requires signal transmittance from the infected tissue to the systemic tissue that usually includes the leaves above the infected tissue. SA is considered a signalling molecule that passes through tissue because its function is to induce the plant defence response. SA is found in the phloem of infected plants, where it moves systematically (Durrant and Dong, 2004). Although SA is a fundamental element of SAR, it is not a systemic signal transmitted by air (Koo et al. 2007; Park et al. 2007; Chen et al. 2003). The systemic transmitting compound is MeSal, which can be converted back to SA through esterase, salicylic acid-binding protein 2 (SABP2). Thus, MeSal is useful as a volatile signalling molecule that facilitates effective long-distance transport of the defence signal.

Fig. 1 illustrates the negative regulation of plant systemic defence

Table 1
Critical literature reviews on sensing technologies and target markers of relevance to future systems addressed to plant protection.

Scope of the review	Ref
Multisensory systems and mathematical models for analysing odour clouds of infochemicals from plants and animals.	Ivaskovic et al. (2021)
Technologies for sampling and analysing total volatile organic compounds emissions from plants in the belowground environment.	Tholl et al. (2021)
Nanomaterials properties and their capabilities to incorporate biomolecules that enable the use of biosensors on plant pathogen detection.	Cardoso et al. (2021)
Chemical sensors used in small drones and their applications to map, localize and identify gases in the environment, industry, or agriculture.	Burgués & Marco (2020)
The role of MeSal emitted by plants and its contribution to the resilience of entire plant communities via volatile plant-to-plant communication.	Singewar et al. (2021)
New trends of MeSal detection with miniaturized sensors that can be adapted to plant protection and agroindustry.	This work

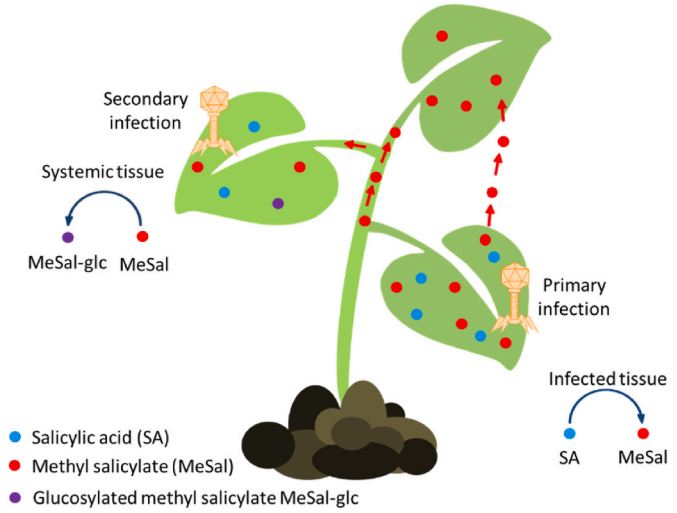

Fig. 1. Development of negative regulation of plant systemic defence and homeostasis of salicylic acid (SA) and methyl salicylate (MeSal) in infected plants.

through MeSal glucosylation. This figure shows that upon infection, the MeSal level increases rapidly in the primary infected tissue. During this process, communication between local and systemic tissue is crucial for SAR activation. The homeostasis of SA and MeSal plays a crucial role. MeSal glycosylation is thus enhanced, resulting in a smaller amount of MeSal being transported to the uninfected systemic tissues. The glucosylation of MeSal in systemic tissue (because MeSal currently has no role in the systemic tissue) to form MeSal-glc ensures that less MeSal is converted to SA. The glucosylation of MeSal therefore adjusts the homeostasis of SA and MeSal and prevents the accumulation of MeSal and further competition with SA (Shulaev et al. 1997; Rowen et al. 2017; Mishina and Zeier, 2007).

3. (Bio)chemical sensors for MeSal

To date, the literature has reported a limited number of (bio)chemical sensors based on electrochemical, conductometric, mass-sensitive, microwave, and spectrophotometric principles to sense MeSal in the vapour or liquid phase. Some of these sensors have demonstrated the ability to detect the concentration levels relevant to plant protection, although without a specific target application or aiming to other application fields, for instance, security/defence (Adams et al. 2019; Pavey et al. 2012; Rosser et al. 2015) and the food industry (Kakoty and Bhuyan, 2018; Bhattacharyya et al. 2012). However, despite the potential of (bio)chemical sensors and nanomaterials in agriculture and particularly in plant protection via VOC markers, such as MeSal, research in this area is still marginal (Cardoso et al. 2022). Hence, there is interest in furthering (bio)chemical sensing technologies for MeSal monitoring. The following subsections provide an account of the literature materials and concepts used to improve the response and sensitivity of different (bio)chemical sensors to MeSal.

3.1. Electrochemical sensors

Electrochemical sensors have been frequently applied in ambient gas monitoring due to their features, including low energy consumption, high resolution, and sufficient sensitivity. In addition, electrochemical sensors are promising candidates for point of care (PoC) to the greatest extent possible (Zhang et al. 2020), can be integrated with complementary elements (e.g., microfluidics and digital technologies), can incorporate self-powered concepts, and can be produced at a low cost using emerging micro-/nanofabrication technologies (e.g., flexible substrates, nanomaterials, bioreceptors) (Campuzano et al. 2021). Electrochemical devices have even been used as wearable gas sensors due to their robustness (Yi and Xianyu, 2022). However, research on electrochemical gas sensors still aims to overcome several challenges, such as high-temperature stability and finding an adequate platform and materials for mass production. For instance, nanotubes (Cao and Rogers, 2009), conductive polymers (Hamilton et al. 2005; Tomić et al. 2021), and metal organic frameworks (MOFs) (Tomić et al. 2021; Kumar et al. 2019) have been used on electrodes. Furthermore, the application of ionic liquids (ILs) in gas sensing instead of conventional electrolytes allows circumventing the gas separating membrane (Silvester, 2011). Additionally, ILs possess a broad potential window and high thermal stability.

The key function in electrochemical sensors is electron transfer between the electrode and the targeted species, which occurs in the interfacial layer. The sensitivity and subsequently the LOD are influenced by several parameters, including the kinetics of charge transfer, the diffusion coefficient of the target species, and the degree of accumulation of the target species on the electrode surface, which can be modulated by using physical and chemical modification (Bakker and Qin, 2006).

Sensitive electrochemical detection of MeSal was achieved previously by using a carbon screen-printed electrode (SPE) modified with gold nanoparticles (NPs) (20 nm) (Umasankar and Ramasamy, 2013). The evaluation of this system in an alkaline solution (0.1 M, NaOH) showed two oxidation peaks at the gold electrode, which appeared at +0.3 V and +0.5 V. The observed oxidation peaks corresponded to the adsorption of gold hydroxide and the formation of gold oxide at the gold surface based on eqs. (1)–(3)

$$Au + OH^- \rightarrow AuOH_{ads} + e^- \quad (1)$$

$$2\,OH^- \rightarrow H_2O + 2\,e^- + \frac{1}{2}\,O_2 \quad (2)$$

$$3\,O_2 + 4\,Au \rightarrow 2\,Au_2O_3 \quad (3)$$

Upon the addition of MeSal into the measuring solution, it was hydrolysed to methanol and salicylate dianion, as described in eq. (4). Indeed, methanol was adsorbed on the gold electrode to form $AuCH_2OH$, which was subsequently oxidized to formaldehyde, as described in eq. (5). On the other hand, the salicylate dianion could also be adsorbed on the gold surface and undergo oxidation to quinone, as shown in eq. (6).

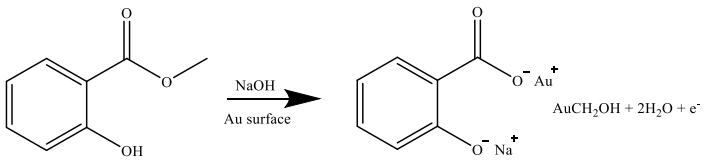

$$AuCH_2OH \rightarrow CH_2O + H^+ + e^- \quad (5)$$

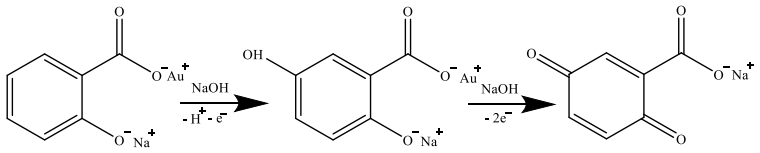

Hence, the electrochemical oxidation of MeSal was catalysed by $AuOH_{ads}$ and Au_2O_3, which were converted back to Au through the catalytic cycle. The reported sensitivity for the developed Au NP-modified carbon SPE was determined to be 127.23 μA mM^{-1} using cyclic voltammetry and 61.04 μA mM^{-1} using differential pulse voltammetry (DPV). The selectivity of the developed sensor was investigated in the presence of green leaf volatiles, including *cis*-3-hexenol, hexyl acetate, and *cis*-hexenyl acetate, and no significant interference with MeSal detection was found. These sensors were successfully applied for MeSal determination in soybean pod extract.

The electrochemical detection of MeSal was also realized by using electrodeposited nano-spinel cobalt oxide (Co_3O_4) films (Kanagasabapathy et al. 2015). The prepared film was employed for the anodic oxidation of MeSal while chronopotentiometry and chronopotentiometry transients were recorded. As reported, the anodic oxidation of the prepared (Co_3O_4) film along with the use of 0.25 M KOH increased the hydrolysis rate of MeSal. It was suggested that the oxidation mechanism involves four electrons; the conversion of salicylate dianion to 1,2-benzoquinone (B) was preferred over that to 1,4-benzoquinone derivative (A), Fig. 2. Based on chronopotentiometric transient analysis, the MeSal concentration was correlated to the consumed charge, which subsequently corresponded to the time duration of the applied anodic current. The LOD was reported to be 2.0×10^{-4} M for MeSal determination. However, the developed method was not applied in real sample analysis.

MeSal detection in pharmaceutical formulations was also achieved by anodic oxidative chronopotentiometric transients in galvanostatic mode at a graphite pencil anode (Kanagasabapathy et al. 2014). In that study, the anodic potential shifted cathodically with MeSal concentration. Because of its slow electron transfer characteristic, salicylate

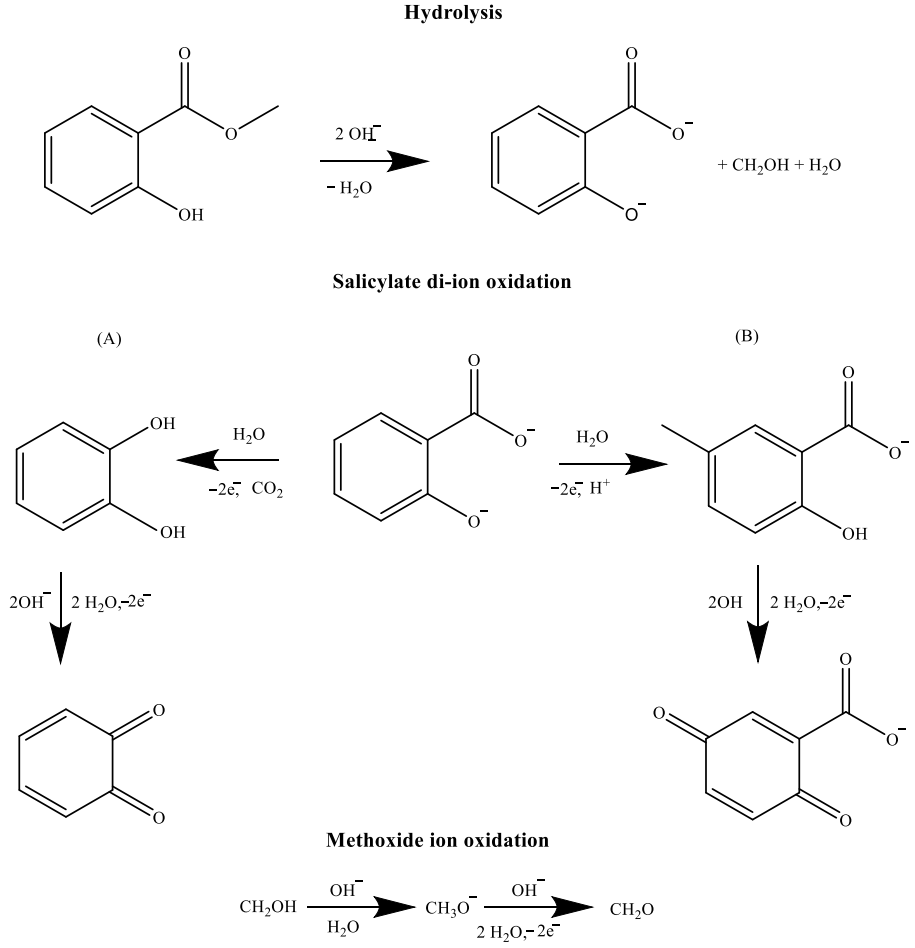

Fig. 2. Anodic electron transfer scheme for MeSal oxidation. Adapted with permission from reference (Kanagasabapathy et al. 2015). Copyright 2015: Elsevier.

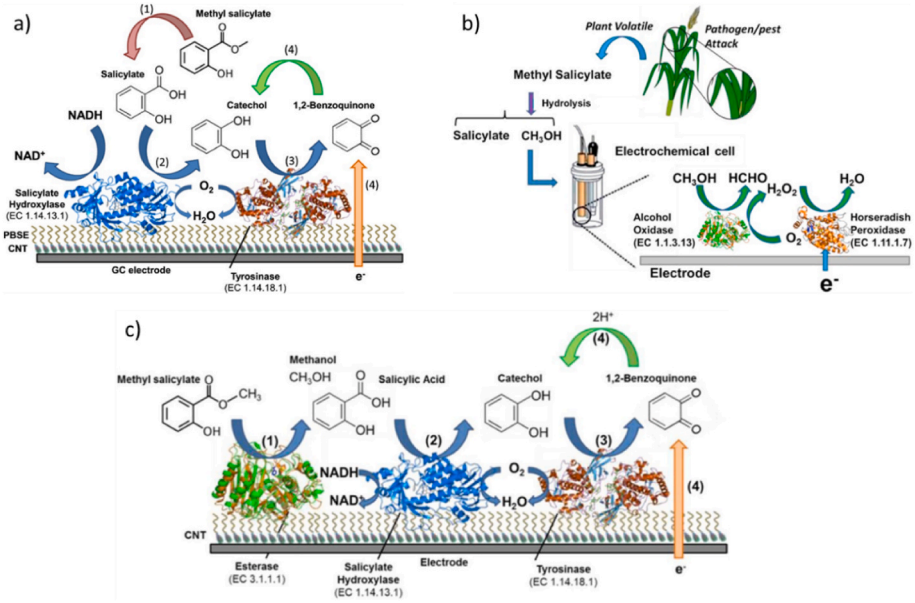

Fig. 3. a) Mechanism of action of the bienzyme electrochemical biosensor containing SH and TYR for the detection of MeSal. **b**) Mechanism of action of the bienzyme electrochemical biosensor containing alcohol oxidase and horseradish peroxidase (HRP) for the detection of MeSal. **c**) Mechanism of action of the trienzyme-based electrochemical biosensor containing esterase, SH, and TYR for the detection of MeSal. Adapted with permission from references (Fang et al., 2016a) (Copyright, 2016: Elsevier) (Fang et al., 2016b), (Copyright, 2016: Elsevier), and (Fang et al. 2018) (Copyright, 2018: IOP Publishing Ltd).

dianion oxidation was affected by the activation polarization. Benzoquinone was formed as the oxidation product. The anodic shift in the oxidation potential was increased in the presence of diclofenac. Nonlinear best-fit models were applied to correlate the anodic potential with the anodic current and MeSal concentration. The results indicated an LOD of 7 mM and a negligible absolute error of 0.005. The application of a graphite pencil electrode as the anode avoided any electrode preparation step and consequently simplified this procedure.

3.1.1. *Electrochemical enzyme-based biosensors for the detection of MeSal*

Biosensor function is based on a specific recognition event occurring between an analyte and a key element called a bioreceptor. This recognition event causes a change in the physiological properties of the substrate or the generation of a product that generates an electrochemical signal such as potential, current, or impedance. Sometimes, to obtain an electrochemical signal from a target analyte, it is required to utilize two or even more enzymes, with the analyte of interest undergoing subsequent enzymatic reactions (cascade reactions) to finally be converted to an electrochemically detectable product (Nguyen et al. 2019). This concept was used for MeSal detection by employing enzyme cascade reactions, in which the hydrolysed form of MeSal, i.e., salicylate was converted to catechol by salicylate hydroxylase (SH) in the presence of nicotinamide adenine dinucleotide (NADH) and oxygen (Fang et al., 2016a). To achieve higher selectivity, the generated catechol was oxidized enzymatically to 1,2-benzoquinone by tyrosinase (TYR). Finally, the electrochemical reduction of the produced 1,2-benzoquinone to catechol was used as the analytical signal (Fig. 3a).

The glassy carbon electrode (GCE), used as the transducer, was modified with multiwalled carbon nanotubes (MWCNTs) by drop casting. The addition of a solution of 1-pyrenebutanoic acid succinimidyl ester (PBSE) to the MWCNT-modified GCE provided appropriate sites for covalent bonding with the enzymes, leading to stable enzyme immobilization. A volume of the solution containing the SH and TYR enzymes was added to the surface of the prepared MWCNTs and incubated to allow the formation of covalent bonds between the PBSE and enzyme. The sensitivity of the developed biosensor was reported to be 30.6 mA cm^{-2} mM^{-1}, while the LOD and limit of quantification (LOQ) were calculated to be 0.0137 μM and 0.0390 μM, respectively. The accuracy of the method was verified by the analysis of the synthetic samples representing the healthy and aphid-infected soybean plants, where the current response was observed only in the presence of the latter sample.

Similarly, another work reported a bienzymatic biosensor composed of alcohol oxidase immobilized on MWCNT/GCE by covalent bonding using PBSE (Fang et al., 2016b). In this approach (Fig. 3b), MeSal underwent hydrolysis in KOH to form salicylate and methanol. The latter was oxidized to formaldehyde, generating H_2O_2 as a byproduct. The enzymatic reduction of the generated H_2O_2 to H_2O was realized by horseradish peroxidase (HRP), and the cofactor was oxidized. The oxidized cofactor could be reduced by electron exchange with the electrode, generating the analytical signal in amperometric measurements. The sensitivity, LOD, and LOQ were reported to be 282.82 μA cm^{-2} mM^{-1}, 0.98 μM, and 2.97 μM, respectively. The developed sensor was successfully applied for the determination of MeSal in macerated wintergreen oil. MeSal, as the main component of wintergreen oil, is produced when stress is induced to the plant's leaves by placing them in warm water.

A more practical biosensor for the sensitive determination of MeSal

Table 2
Summary of reports on electrochemical sensors for MeSal detection.

Principle	Receptor	Tested concentration	Sensitivity	LOD	T	Ref.
CV-DPV	Au NPs-SPCE	62–1700 μM	127.23 μA cm^{-2} mM^{-1}	39.44 μM	RT	Umasankar & Ramasamy (2013)
CP	Nano-spinel Co_3O_4 film	3–11 μM	N/A	200 μM	RT	Kanagasabapathy et al. (2015)
CP	Graphite pencil electrode	7–42 mM	N/A	7 mM	RT	Kanagasabapathy et al. (2014)
Amp.	SH, Tr/CNT	0–27.8 μM	30.6 μA cm^{-2} μM^{-1}	0.14 μM	RT	Fang et al. (2016a)
Amp.	AOx, HRP/CNT	0–100 μM	282.82 μA cm^{-2} mM^{-1}	0.98 μM	RT	Fang et al. (2016b)
Amp.	Esterase, SH, Tr/CNT	0–27.8 μM	1.55 μA cm^{-2} mM^{-1}	0.7 μM	RT	Fang et al. (2018)

LOD: limit of detection. T: temperature. CV-DPV: cyclic voltammetry - differential pulse voltammetry. CP: chronopotentiometry. Amp.: amperometry. NPs: nanoparticles. SPCE: screen-printed carbon electrode. SH: salicylate hydroxylase. Tr: tyrosinase. CNT: carbon nanotube. AOx: alcohol oxidase. HRP: horseradish peroxidase. RT: room temperature (24–29 °C).

Table 3
Summary of reports on conductometric, mass-sensitive, and microwave sensors for MeSal detection.

Principle	Receptor	Tested concentrations	Response to maximum tested concentration	LOD	T	Ref.
Conductometric sensors						
Resistive	SnO_2-Pt	20 ppm	$\Delta R/R_0 = 70\%$	N/A	350 °C	Bhattacharyya et al. (2012)
Resistive	SnO_2-Ag	N/A	$\Delta V/V_0 = 65\%$	N/A	150 °C	Kakoty & Bhuyan (2018)
Capacitive	ADIOL	0.3–1 ppm	$C/C_0 = 0.6\%$	N/A	RT	Patel et al. (2008)
LCR	Au NPs-A3 peptide	6–12 ppm	$F_1 = 75$ kHz	N/A	N/A	Nagraj et al. (2013)
FET	Gr-LBN with MSP	1 fM–10 nM	$\Delta I/I_0 = 14\%$	N/A	RT	Murugathas et al. (2020)
Mass-sensitive sensors						
QCM	MDEX	10–900 ppm	$F_{dev} = 110$ Hz	N/A	RT	Sharma et al. (2016)
Microwave sensors						
MW-Ant	Gr- MIP (polyphenol)	10–200 ppt	$S_{11}/(S_{11})_0 = 140\%$	N/A	RT	Adams et al. (2019)

LOD: limit of detection. T: temperature. LCR: inductor-capacitor-resistor. FET: field effect transistor. QCM: quartz crystal microbalance. MW-Ant: microwave antenna. ADIOL: bis[(*E*)-1,1,1-trifluoro-2(trifluoromethyl)pent-4-en-2ol]siloxane. Gr: graphene. LBN: lipid bilayer nanodiscs. MSP: membrane scaffold protein. MDEX: maltodextrin. MIP: molecularly imprinted polymer. *R*: resistance. *C* = capacitance. F_1: resonant frequency of the imaginary part of the resonance impedance spectrum. F_{dev}: frequency deviation. *I*: current. S_{11}: reflection coefficient spectrum. RT: room temperature (24–29 °C).

was developed using the concepts described above. In this new development, the hydrolysis of MeSal was carried out by esterase (Fang et al. 2018), so the hydrolysis of MeSal in KOH solution and further pH adjustment were not needed. Similarly, the MWCNT/GCE was prepared and immobilized with a mixture containing esterase, SH, and TYR. The four cascade reactions included the hydrolysis of MeSal to SA by esterase, conversion of produced SA to catechol by SH and enzymatic oxidation of catechol to 1,2-benzoquinone by TYR. The generated 1, 2-benzoquinone could be reduced back to catechol by electron transfer with the electrode, and the amperometric current response was applied as the analytical signal (Fig. 3c). It was shown that the hydrolysis reaction of MeSal catalysed by the esterase is the rate-limiting step in the cascade reactions. The sensitivity, LOD, and LOQ were calculated to be 1.55 μA cm^{-2} mM^{-1}, 0.7 μM, and 2.1 μM, respectively. Table 2 summarizes the main characteristics of the electrochemical sensors used for MeSal determination. Even though a higher sensitivity and a lower LOD were reported for this trienzyme-based biosensor than for the bienzyme biosensor, the former was not applied in the analysis of real samples.

3.2. Conductometric sensors

Conductometric-based chemical sensors are usually represented by bipolar devices that measure the electrical resistance, capacitance, and/or impedance changes of the active sensing material (receptor) in DC or AC mode. However, these types of sensors may also come in different configurations, for instance, with a third electrode, to allow the device to operate as a field-effect transistor (FET). In this configuration, the third electrode, also known as the gate electrode, tunes the electrical field within the active sensing material, allowing the modulation of its conductivity (Janata, 2009; Grundler and Janata, 2008).

Conductometric sensors based on resistive, capacitive, and FET principles have been used successfully to detect MeSal both in the liquid and vapour phases, as summarized in Table 3. Traditional resistive sensors, for instance, have shown a response to MeSal using SnO_2 modified with various materials, including Ag, Pt, Au, CuO, CaO, PdO, and Fe_2O_3 (Bhattacharyya et al. 2012), as receptor elements. The operation of these sensors at high temperature (350 °C) suggested an improved response, particularly for the structures modified with Ag and Pt, which displayed responses of 68 and 70% to 20 ppm of MeSal in the vapour phase. A recent study on SnO_2 modified with Ag also corroborated the sensitivity of this material to MeSal, although the report did not specify the range of concentration and the LOD for this compound (Kakoty and Bhuyan, 2018).

Capacitive sensors based on polymers have also shown a response to MeSal (Fig. 4a). These sensors based on multiple polymers, including polyisobutylene (PIB), poly(ethylene-co-vinyl acetate) (PEVA), bis[(E)-1,1,1-trifluoro-2-(trifluoromethyl)pent-4-en-2-ol]siloxane (ADIOL), and polyepichlorohydrin (PECH), with different dielectric constants, capacitances, and relative chemical polarities were used successfully to detect MeSal in capacitive mode (Patel et al. 2008). Studies of these four polymers revealed temperature-dependent responses with significant changes upon 5 °C steps. The results showed that the most successful system in terms of selectivity involved ADIOL, a polymer with a dielectric constant of 5.3 and polar and hydrogen-bond acidic properties. This system displayed a response to MeSal in the range of 0.3 to 1 ppm at 25 °C, although the response rate was lower at this temperature and the humidity interference was stronger than those of the other polymers tested (e.g., PIB, PEVA, and PECH).

The use of a multivariable inductor-capacitor-resistor (LCR) resonator based on a flexible substrate and peptide-caped gold NPs was also evaluated for MeSal (Fig. 4b) (Nagraj et al. 2013). These systems were tested using inductively coupled measurements of the resonant impedance while exposing the sensors to MeSal so that the resonance

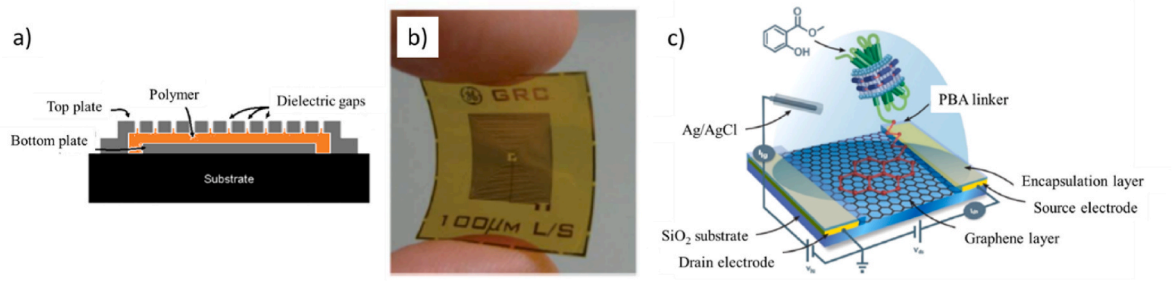

Fig. 4. a) Scheme of a polymer-filled capacitive sensor, **b)** photograph of a multivariable inductor-capacitor-resistor (LCR) resonator based on Kapton, **c)** scheme of an FET sensor based on insect odourant receptors and liposomes immobilized on a graphene layer. Adapted with permission from references (Patel et al. 2008) (Copyright, 2008: Elsevier) (Nagraj et al. 2013), (Copyright, 2013: Royal Society of Chemistry), and (Murugathas et al. 2020) (Copyright, 2020: American Chemical Society), respectively.

impedance spectra provided several parameters, such as the frequency position and magnitude of the real part of the impedance and the resonant/antiresonant frequencies and their magnitudes from the imaginary part of the impedance. These sensors detected MeSal in a concentration range from 6 to 12 ppm, showing a significant response in the resonant frequency (~75 kHz) of the imaginary part of the impedance and the magnitude (~0.5 Ω) of the real part of the impedance to 12 ppm MeSal. The multivariable analysis of the measurements and the specific A3 peptide (AYSSGAPPMPPF) employed as the active sensing element allowed a single sensor to discriminate the response of MeSal, acetonitrile, and dichloromethane, despite the similar dielectric constants of MeSal ($\epsilon_r = 9.0$) and DMC ($\epsilon_r = 9.1$).

The FET configuration, in which insect odourant receptors (ORs) and liposomes are immobilized on a graphene layer, has also been evaluated to detect low MeSal concentrations (from 1 fM to 10 nM) (Murugathas et al. 2020). The evaluation included different active sensing elements, including two ORs from *Drosophila melanogaster* integrated into nanodiscs (10–20 nm diameter) composed of a lipid bilayer enclosed in a membrane scaffold protein as well as the same ORs with OR coreceptor subunits (ORco) cointegrated in the lipid bilayer. These systems (Fig. 4c) employed a liquid-gate configuration in which an electrolyte and Ag/AgCl standard electrodes were used as the gate electrode. The results displayed better sensitivity for the sensors based on OR integrated into the nanodiscs compared to the other active sensing elements studied, showing a change in the drain-source current of 0.14 to 10 nM MeSal.

3.3. Mass-sensitive sensors

Mass-sensitive sensors are based on the piezoelectric effect. These types of sensors utilize piezoelectric quartz crystals as transducers coated with an active sensing layer capable of absorbing gaseous/vapour analytes. The mass changes produced by the absorbed species are generally measured as frequency shifts by electrical oscillator circuits (Janata, 2009; Grundler and Janata, 2008). In the past, mass-sensitive sensors, usually based on thickness-shear mode resonators, surface acoustic waves, and cantilevers, proved to be sensitive to various gases and vapours (Oprea & Weimar 2020), including MeSal (Sharma et al. 2016). In particular, MeSal detection was achieved by using quartz crystal microbalances (QCM, a type of thickness-shear mode resonator) coated with maltodextrin (MDEX, a polysaccharide used as additive in food), Table 3. These sensors showed a comparatively higher response to MeSal among other aromas, such as linalool, geraniol, linalool oxide, and trans-2-hexanal, in a range of concentrations between 10 and 900 ppm. The results show an adequate correlation (0.982) of the sensor response and the gas chromatography–mass spectrometry estimations made for the analytes in various black tea samples, demonstrating the appropriateness of the sensor to determine MeSal. These systems operated at room temperature and showed high reproducibility, particularly for MeSal concentrations above 500 ppm.

3.4. Microwave sensors

Microwave sensors are based on propagative structures (to transmit the microwaves) integrated with a sensitive material that changes its permittivity as a function of the target analyte and the frequency range of the incident electromagnetic waves (De Fonseca et al. 2015). Hence, the target analyte is detected by measuring the variations in the transmitted and reflected microwaves at discrete frequency intervals. The use of microwave sensors in the gas-sensing field is not as extensive as that of other types of sensors, e.g., conductometric or mass-sensitive sensors. Nevertheless, this technology has already shown sensitivity to various gases and vapours using a variety of sensitive materials (e.g., oxides, zeolites, polymers and carbon-based materials) and propagative structures (e.g., microstrip lines, coplanar waveguides, planar active resonators, and antennas) (Li et al., 2019d). Their use for MeSal detection was reported in the past based on an antenna propagative structure with molecular imprinted polymer (MIP)-functionalized graphene as a sensitive material (Adams et al. 2019), Table 3. Generally, MIPs are synthetic polymers containing tailored recognition sites, which are formed by introducing molecular templates during the polymerization or polycondensation of the polymer's bulk that are later removed to generate cavities shaped for the target molecules (Chen et al. 2016; Arabi et al. 2021). Thus, the MIP-graphene-based antenna system reported previously (Adams et al. 2019) used molecular imprinting technology to trap MeSal in the MIP cavities (Fig. 5) and led to a transfer of electrons to the graphene film through the MIP. Such a structure proved to induce changes in the electrical resistance and reflection coefficient of graphene, which were subsequently transduced in impedance changes of the antenna. The antenna sensing system exhibited sensitivity to MeSal at the ppt level and room temperature, with high selectivity to MeSal over other vapours, such as acetone and water. This ultrahigh sensitivity was attributed to the two-dimensional graphene film, which exhibits notable relative changes in carrier concentration even when few electrons participate in the MeSal-MIP interactions. The selectivity, in contrast, was attributed to the MIP based on polyphenol, which provides cavities tuned in shape and size to the target molecule (or similar molecules) with the adequate functional monomer orientation at these cavities that allow binding only the target molecules. Molecular imprinting technology has also been used in the past to improve the selectivity to other vapours, such as formaldehyde (Tang et al. 2017;

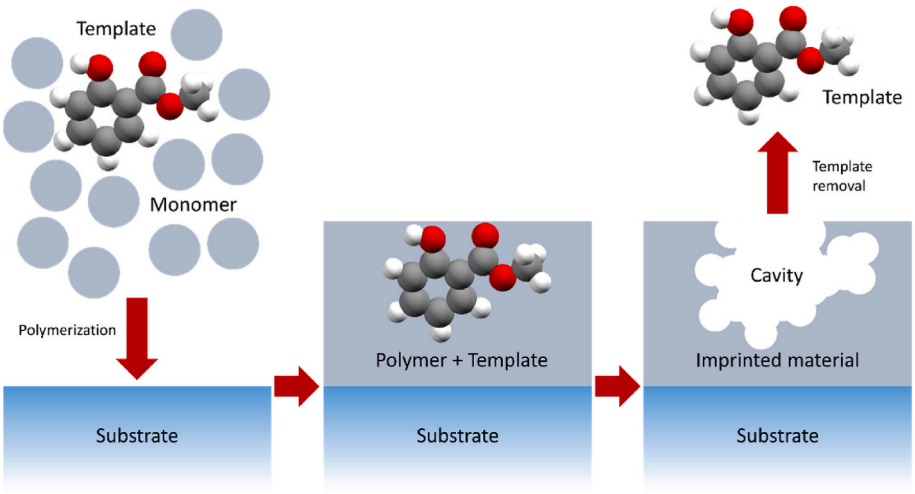

Fig. 5. Illustration of the processing steps to form a molecular imprinted polymer film with MeSal as the molecular template.

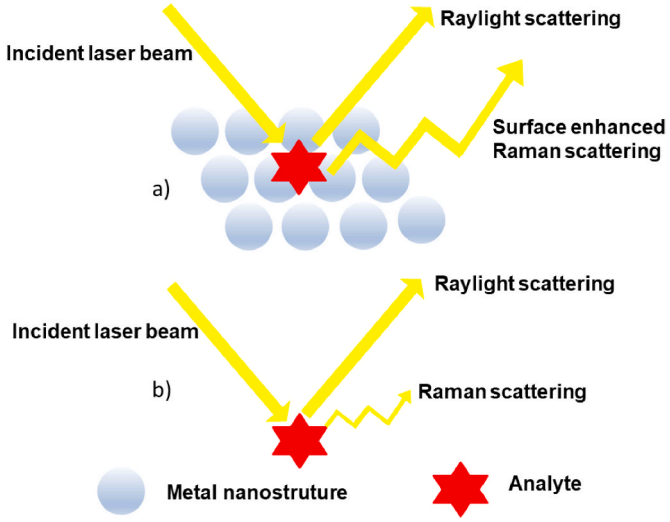

Fig. 6. Schematic illustration of the principle of surface-enhanced Raman spectroscopy. a) Effect of the presence of the metal nanostructures on the enhanced intensity of Raman scattering and b) the low intensity of Raman scattering obtained by the analyte without using metal nanostructures.

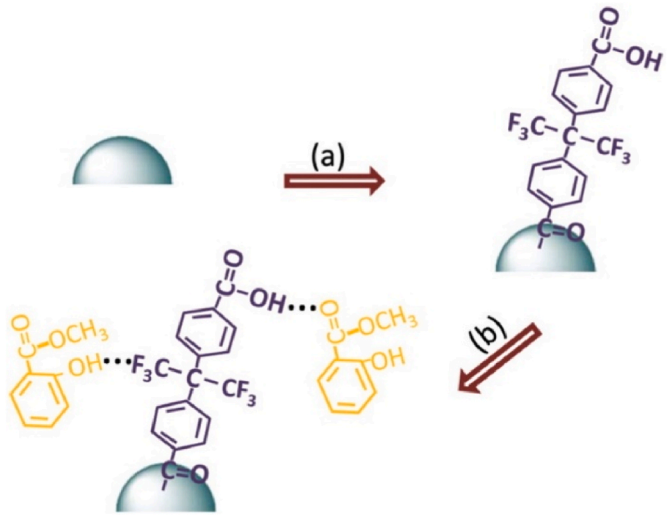

Fig. 7. The fabrication process of linker molecule-assisted assembly complex for SERS detection, a) immobilization of the linker and b) bonding of the linker and MeSal. Adapted with permission from reference (Li et al. 2018). Copyright 2018: Elsevier.

Zhang et al. 2014), methanol (Zhu et al. 2015), and nitrobenzene (Alizadeh and Hamedsoltani, 2014). This technology has proven to have good stability and selectivity, although the dynamics of the response were reported to be slow due to the binding/elution process between the target molecules and the MIP, a process that can last a significant time (Zhang et al. 2017).

3.5. Spectrophotometric sensors

3.5.1. Surface-enhanced Raman scattering sensors

Surface-enhanced Raman scattering (SERS) has recently emerged as an important analytical technique for different analytes, including clinical biomarkers (Song et al. 2020) and environmental pollutants (Li et al. 2014). This technique is advantageous because it can significantly improve the inherent small Raman scattering cross-section or intensity of molecules because of the tunable signal transduction via the physicochemical properties of plasmonic nanostructures, which are potential materials for SERS substrates. The Raman scattering in SERS is amplified by two mechanisms (Fig. 6). The first is the localization of optical fields in metallic nanostructures, which leads to electromagnetic-field enhancement. Indeed, light accumulates in the gaps, crevices, or sharp features of plasmonic materials, including noble and coinage metals (e.g., silver, gold, and copper) with nanoscale features. The second is the chemical or electronic enhancement caused by the expansion of the Raman cross-section provided when the molecule or lattice is in contact with metal nanostructures (Pilot et al. 2018). The amplified signal, miniaturization capability, rapid response and simple sample preparation make SERS a relatively cost-efficient alternative platform for conventional MeSal analysis (Park et al., 2020a; Li et al. 2018; Park et al. 2019; Park et al., 2020b).

Previously, the detection of MeSal based on SERS was carried out by introducing the reagent 4,4′-(hexafluoroisopropylidene)bis(benzoic acid) as a capturing assistant to form a MeSal/assistant/Ag NP system (Fig. 7a) (Li et al. 2018). In fact, the CF_3 group, which is a strong electron withdrawer in the assistant molecule, forms strong hydrogen bonds. In the proposed mechanisms, the carbonyl group of MeSal and the hydroxyl group of the assistant molecules can couple, or the hydroxyl of MeSal and the fluorine of the assistant molecules can couple (Fig. 7b). The minimum detection concentration for this system was reported to be 10^{-4} M, although it was not tested in the analysis of real samples.

Another work proposed bringing Ag nanospheres (NSs) to the aqueous phase from the nonaqueous phase by using the cationic surfactant tetraoctylammonium bromide (TOAB). The complex formed between the Ag NSs and Tenax-TA adsorbent polymer was capable of collecting volatile MeSal. The formed complex was used as a SERS substrate to determine MeSal after 4 h of collecting this volatile. The authors stated that among the three cationic surfactants investigated (TOAB, cetyltrimethyl ammonium bromide (CTAB), and benzalkonium chloride (BKC)), the phase transfer of the Ag NSs occurred only when using TOAB. The proposed mechanism includes electrostatic interactions induced by TOAB surfactants. The key success of this approach was to use an aggregate covered by surfactants with an enlarged surface area (Park et al. 2019). The real sample analysis was not reported.

Recently, a Raman-based VOC detection system based on signal differentiation by multivariate analysis was also developed (Park et al., 2020a). In this work, a small volume of four representative VOCs (linalool, *cis*-3-hexenyl acetate, *cis*-3-hexen-1-ol, MeSal) were preconcentrated by using Hayesep Q adsorbent in a sealed chamber (Fig. 8). Raman spectroscopy (RS) was performed to quantify the VOC eluates from each adsorbent after an adequate collection time. As reported after 20 min of collection, unique spectral features were observed in individual and mixed volatiles, indicating good discrimination between VOCs generated by multivariate techniques. Application of Ag nanocrystals (NCs) as the SERS substrate enhanced the sensitivity of the developed method, particularly in the case of MeSal. The developed method was successfully applied for the determination of VOCs in tea samples, indicating its accuracy.

Three different VOCs (linalool, *cis*-3-hexen-1-ol, and MeSal) were detected by SERS in tea samples and cotton plants by using Tenax-TA deposited on a layer of Ag NSs as the SERS substrate and performing Raman data processing by multivariate analysis. The developed method was used successfully for the analysis of VOCs either in dried or live cotton plants (Park et al., 2020b). Table 4 summarizes the main characteristics of the SERS sensors used for MeSal determination.

3.5.2. Colorimetric sensors

Colorimetric sensors are part of the group of optical sensors in which the analytical signal is the colour change of the active sensing element when it is influenced by an external stimulus (e.g., gas/vapour chemical analyte). In this type of sensor, the light absorbed/emitted by the active sensing element is directly proportional to the concentration of the

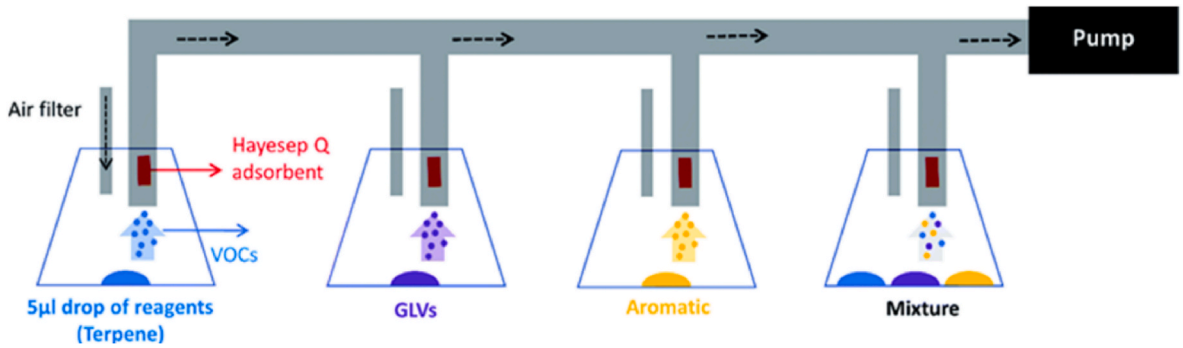

Fig. 8. Scheme of the experimental setup and the parallel VOC collection system. GLVs (green leaf volatiles). Adapted with permission from reference (Park et al. 2020a,b). Copyright 2020: Royal Society of Chemistry.

Table 4
Summary of reports on spectrophotometric sensors for MeSal detection.

Principle	Receptor	Concentration	Response to the maximum concentration tested	LOD	T	Ref.
SERS	assistant/Ag NPs**	N/A	N/A	100 µM	RT	Zhang et al. (2017)
SERS	TOAB/Ag NPs	N/A	N/A	N/A	RT	Song et al. (2020)
SERS	Ag NCs	0.2–4 µg mL^{-1}	N/A	0.2 µg mL^{-1}	RT	Park et al. (2020a)
SERS	Ag NSs	N/A	N/A	N/A	RT	Li et al. (2014)
Colorimetric	$Fe(NO_3)_3$	10–939 ppm	$Rf/Rf_0 = 12000$	N/A	RT	Pavey et al. (2012)
Colorimetric	$Fe(NO_3)_3$	1–10 ppm***	N/A	N/A	RT	Rosser et al. (2015)

LOD: limit of detection. T: temperature. SERS: surface-enhanced Raman spectroscopy. NPs: nanoparticles. NCs: nanocrystals. NSs: nanospheres. *Rf*: reflectance, M: measured, RT: room temperature (24 – 29 °C), **: assistant molecule: 4,4'-(hexafluoroisopropylidene)bis(benzoic acid). ***: exposure flight tests, N/A: data not available. RT: room temperature (24–29 °C).

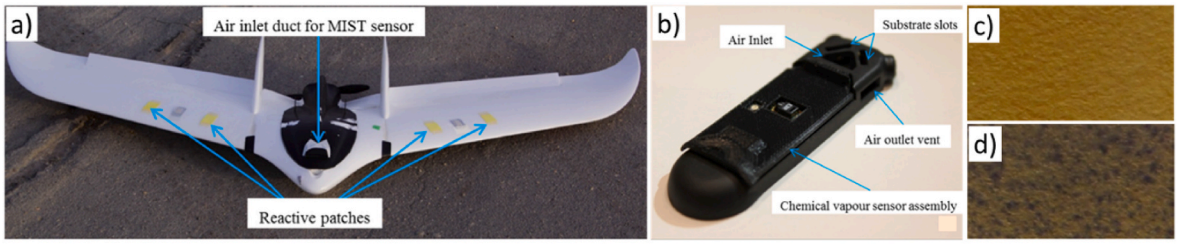

Fig. 9. a) Micro-UAV with the colorimetric sensor and additional chemical detection patches on the leading edge of the wings. **b)** Close view of the sensor assembly embedded in the fuselage of the UAV. Visual inspection of the colour change from **c)** no exposure and **d)** major exposure to MeSal. Adapted with permission from reference (Rosser et al. 2015). Copyright 2015: MDPI.

target analyte (Liu et al. 2020). Usually, these sensors utilize organic compounds as active sensing elements, including dyes, metal organic complexes and polymers, which generally undergo four mechanisms: (i) ring opening and closing reactions, (ii) changes in the functional groups, (iii) ligand exchanges, and (iv) phase transition, in which a colour change is perceived (Cho et al. 2020). Previously, colorimetric sensors have been used to detect various gases and vapours following these principles (Cho et al. 2020). However, due to previous observations on the colour change of complexes with ferric ions exposed to MeSal (Weber, 1977), colorimetric sensors for MeSal have been developed using a relatively simple compound, ferric nitrate, as part of the active sensing element (Table 4). This compound dissolved in

Table 5
Qualitative comparison of the main characteristics and sensing technologies for MeSal.

Properties	Sensors				
	Electrochemical	Conductometric	Mass-sensitive	SERS	Colorimetric
Conc. range of responses	Highly sensitive and broad conc. range. Measurements in gas phase are reported.	Very good sensitivity, but the conc. range is narrow. Measurements in gas phase are reported.	Good sensitivity and for a broad conc. range. Measurements in gas phase are reported.	Very good sensitivity for a broad conc. range. Measurements in gas phase are reported.	Good sensitivity for a broad conc. range. Measurements in gas phase are reported.
Selectivity	Highly selective by using enzymes as bioreceptors.	Some extent of selectivity reached by using selective receptors, such as olfactory receptors, MIP technology.	Some extent of selectivity reached by using selective receptors based on MIP technology.	Some extent of selectivity reached by selectively analytes capture.	The reports do not evaluate their selectivity.
Size	Further miniaturization is required.	Small and compatibility with microfabrication processes.	Small and compatibility with microfabrication processes.	Further miniaturization is required	Small and compatibility with microfabrication processes.

Conc.: Concentration.

dimethylacetamide (DMAc) and coated over a paper-based substrate displayed responses to MeSal in the liquid and vapour phases (Pavey et al. 2012). Further studies of these elements (i.e., ferric nitrate-coated papers) integrated into a real-time optical sensor network platform attached to a protective suit proved effective in detecting MeSal by optical reflectance at room temperature. The calibration curves of these sensors show considerable changes in reflectance, for instance, 12,000 for 939 ppm and a measured limit of detection of 10 ppm. The application of these sensors in autonomous micro-unmanned aerial vehicles (UAV) was also proposed later (Rosser et al. 2015), Fig. 9. Exposure flight tests with the micro-UAV proved the detection of MeSal in a vapour cloud concentration of 3.7 ppm at a distance of 100 m. These tests did not evaluate the selectivity, so there is no account of possible interfering gaseous species.

4. Challenges and future perspectives

4.1. (Bio)chemical sensors and MeSal

MeSal has been identified as an essential VOC in agriculture and other sectors related to the food industry and security. The current state of the art shows various (bio)sensing strategies for detecting MeSal in concentrations that are relevant to these applications. The most promising sensing technologies generally include sensor-based electrochemical, conductometric, mass-sensitive, or microwave principles due to their functional results and prospects for miniaturization and cost-effective production. Table 5 compares the different sensing technologies for MeSal discussed in this review. This table was compiled based on the reports and data summarized in Tables 1–3 to rate three significant factors of sensory devices, such as the concentration range of responses, selectivity, and size.

The group of electrochemical sensors have exhibited high sensitivity, precision, and accuracy for the detection of MeSal. Further solutions, however, need to be explored to avoid the prehydrolysis step to convert MeSal into salicylate ions to suit practical applications, as addressed previously in a trienzyme-based biosensor (Fang et al. 2018). Other challenges for electrochemical sensors involve the search for solutions that allow further reduction of their dimensions so that their size and power consumption can enable their use in *in situ* analysis.

From the group of conductometric sensors, capacitive and FET systems based on polymers such as ADIOL (with polar and hydrogen-bond acidic properties) or insect odourant receptors (such as those from *Drosophila melanogaster*), respectively, can play a positive role in MeSal sensing. Similarly, mass-sensitive sensors with sensitive elements such as polysaccharide (MDEX) or microwave sensors based on molecular imprinted polymers show promising performance. The use of these technologies and materials in practical applications is subjected to overcoming their long-term stability issues and sensitivity to external factors such as humidity and temperature. Additionally, the modulation of their selectivity by surface functionalization and the search for new solutions based on combinatorial sensing systems are characteristics that need to be addressed further. The intrinsic potential of miniaturization and on-chip integration of this group of sensors, however, opens the possibility of using multivariable signal concepts (sensor arrays with different receptors and principles) for further improvements of selectivity by training and predictive algorithms that recognize chemical patterns and discriminate specific species such as MeSal.

Other possible prospects for MeSal sensing include sensing technologies based on spectrophotometric principles. This group of sensors, represented in particular by SERS, has shown effectiveness in detecting MeSal, although without a clear account of the sensitivity levels and usually incorporating preconcentration steps. However, it seems that the application of SERS-based sensors for MeSal detection is still in its infancy, and more research is needed to evaluate its appropriateness for practical applications.

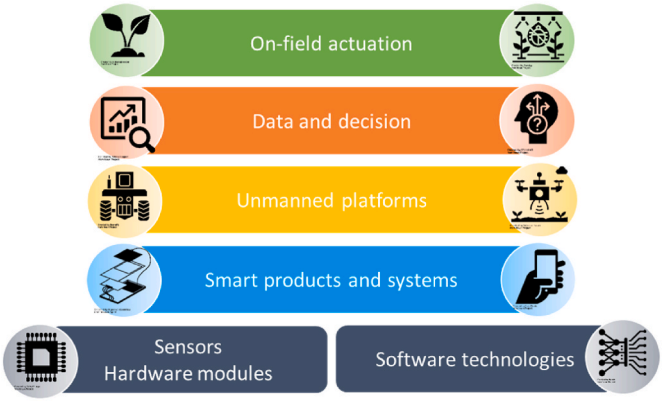

Fig. 10. Value chain for the practical application of technology in agriculture. The cornerstone of this chain involves hardware (e.g., sensors and electronics) and software technologies (artificial intelligence), which are then integrated into smart portable products that can be attached to unmanned agriculture platforms to deliver data supported decisions for more efficient management of the crops.

4.2. (Bio)chemical sensors and agriculture 5.0

Modern agriculture incorporates precision farming concepts, i.e., the use of satellites and autonomous and unmanned vehicles equipped with cameras and sensors that provide useful information for tuning the amount of fertilizers and pesticides in the field and improving crop yields (Saiz-Rubio and Rovira-Más, 2020). For future decades, however, a more global concept based on information collection, analysis of massive data, and the use of robotics and artificial intelligence (AI) will be pursued to enable better management of information and transform this sector into a more knowledge-driven sector. This holistic concept is the core of the so-called *Agriculture 5.0,* which includes not only the 'traditional' precision agriculture principles but also the further use of unmanned operations and autonomous decision support systems with robots, edge computing, and AI (Saiz-Rubio and Rovira-Más, 2020).

Among several key players in the new agriculture era, sensing technologies are still the cornerstone of the value chain (Fig. 10). Modern agriculture already includes sensors to monitor crops and provide data related to the environment and soil. Crop diseases and pest infestation that are visible to the human eye are also controlled to a certain extent by using affordable image (spectral) sensors, although with low resolution. New image sensors based on multispectral or hyperspectral data are an alternative to provide higher resolution, although at higher costs (Yang, 2020; Burgués and Marco, 2020; Saiz--Rubio and Rovira-Más, 2020; Mahlein, 2016; Madufor et al. 2017).

In recent years, (bio)chemical sensors have emerged as an attractive alternative to pest crop prevention owing to the specific VOC produced by infested plants (Jansen et al. 2009, 2011; Ivaskovic et al. 2021). Although these markers can be recognized accurately by classical equipment (e.g., gas chromatography spectrometer) or molecular assays (e.g., nucleic acid-based technologies such as PCR) (Li et al., 2019a; De Lacy Costello et al. 2001), the deployment of such equipment and techniques in the field for agriculture is technically and economically disadvantageous. In this context, (bio)chemical sensors represent a valid alternative to address the challenges of *Agriculture 5.0.* (Bio)chemical sensors have shown highly sensitive features that have contributed to advances in many domains, especially in industry and environmental control. Moreover, they can be miniaturized using today's micro-/-nanotechnologies to further reduce their energy consumption and improve their autonomy in remote applications for noninvasive plant disease diagnostics (Li et al., 2019a; Potyrailo, 2016; Hu et al. 2019). Efforts in the near future for these sensors must concentrate on addressing the specific challenges of the agriculture sector; therefore, possible improvements to pursue include the following:

- Development of new or optimized (bio)chemical receptors to plant health-related VOCs. For instance, heavier compounds with less volatility, such as methyl salicylate, methyl jasmonate, terpene alcohols, and green leave volatiles (e.g., cis-3-hexenal and trans-2-hexenal) as they are more likely to function as signals over long distances and are frequent markers showing changes after the triggering of a disease independent of the plant species.
- (Bio)chemical sensors capable of detecting plant health-related VOCs using noninvasive monitoring concepts, for instance, by measuring markers in the vapour phase at relevant concentration levels.
- Miniaturization and integration of sensors with diverse transducing principles (electrochemical, conductometric, optic, *etc.*) to facilitate integrated multivariable responses (a concept directed to replace conventional single-output sensors and the classical sensor arrays).
- Integration of embedded electronic components, such as nonvolatile memory technologies, enables local processing and storage of data near the sensor (where data are generated) to reduce data traffic and power consumption.
- Further reduction of power consumption below tens of μW to improve sensor autonomy for continuous real-time measurements.

The amount of work that miniaturized and multivariable remote advanced sensors with embedded AI can handle is not comparable to that of traditional monitoring methods. These envisioned VOC monitoring systems for agriculture will reduce to maximum farm work and costs, ensuring sustainable agriculture in the near future.

5. Conclusions

This review summarizes the principles employed for MeSal sensing, providing insight into the receptors or sensitive materials used in combination with these principles and their performance. These technologies showed significant advances for detecting MeSal either in the vapour or in the liquid phase. However, the new developments for noninvasive health monitoring addressed to agriculture and plant protection demand further focus on technologies that enable sensing of MeSal or other key plant volatiles in the vapour phase at ppb level. These new technologies for sensing vapours, including MeSal, must include micro-/nanofabrication concepts for providing miniaturization and portability to these developments, as well as for facilitating multivariable sensing and artificial intelligence concepts. These features would drive the practical application, not yet established, of (bio)chemical sensors in plant protection.

Declaration of competing interest

The authors declare that they have no known competing financial interests or personal relationships that could have appeared to influence the work reported in this paper.

Data availability

No data was used for the research described in the article.

Acknowledgements

This research was carried out under the project CEITEC 2020 (LQ1601) with financial support from the Ministry of Education, Youth and Sports of the Czech Republic under the National Sustainability Program II. The support of MCIN/AEI/10.13039/501100011033 via Grant PID2019-107697RB-C42 is also acknowledged.

References

Abraham, K., Shankaranarayana, M., Raghavan, B., Natarajan, C., 1976. Microchim. Acta 65, 11–15.
Adams, J.D., Emam, S., Sun, N., Ma, Y., Wang, Q., Shashidhar, R., Sun, N.-X., 2019. IEEE Sensor. J. 19, 6571–6577.
Adzib, M.S.M., Ilham, Z., 2020. AIMS Medical Science 7, 43–56.
Alizadeh, T., Hamedsoltani, L., 2014. J. Environ. Chem. Eng. 2, 1514–1526.
Anderson, P.K., Cunningham, A.A., Patel, N.G., Morales, F.J., Epstein, P.R., Daszak, P., 2004. Trends Ecol. Evol. 19, 535–544.
Anyakudo, F., Adams, E., Van Schepdael, A., 2019. J. Pharmaceut. Biomed. Anal. 171, 65–72.
Arabi, M., Ostovan, A., Li, J., Wang, X., Zhang, Z., Choo, J., Chen, L., 2021. Adv. Mater. 33, 2100543.
Ashrafi, A.M., Sys, M., Sedlackova, E., Farag, A.S., Adam, V., Pribyl, J., Richtera, L., 2019. Sensors 19.
Baker, R.H.A., Sansford, C.E., Jarvis, C.H., Cannon, R.J.C., MacLeod, A., Walters, K.F.A., 2000. Agric. Ecosyst. Environ. 82, 57–71.
Bakker, E., Qin, Y., 2006. Anal. Chem. 78, 3965–3984.
Baldwin, I.T., Halitschke, R., Paschold, A., Von Dahl, C.C., Preston, C.A., 2006. science 311, 812–815.
Bhattacharyya, N., Dutta, D., Ghosh, S., Mandal, S., Narjinary, M., Sen, A., Bandyopadhyay, R., 2012. IMCS 2012 – the 14th International Meeting on Chemical Sensors (Nuremberg, Germany).
Burgués, J., Marco, S., 2020. Sci. Total Environ., 141172
Bytesnikova, Z., Pecenka, J., Tekielska, D., Kiss, T., Svec, P., Ridoskova, A., Bezdicka, P., Pekarkova, J., Eichmeier, A., Pokluda, R., Adam, V., Richtera, L., 2022. Chem Biol Technol Ag 9.
Cai, X.-M., Xu, X.-X., Bian, L., Luo, Z.-X., Chen, Z.-M., 2015. Anal. Bioanal. Chem. 407, 9105–9114.
Campuzano, S., Pedrero, M., Yáñez-Sedeño, P., Pingarrón, J.M., 2021. Sensor. Actuator. B Chem. 345, 130349.
Cao, Q., Rogers, J.A., 2009. Adv. Mater. 21, 29–53.
Cardoso, R.M., Pereira, T.S., Facure, M.H., dos Santos, D.M., Mercante, L.A., Mattoso, L. H., Correa, D.S., 2021. Sensors and Actuators Reports, 100068.
Cardoso, R.M., Pereira, T.S., Facure, M.H.M., dos Santos, D.M., Mercante, L.A., Mattoso, L.H.C., Correa, D.S., 2022. Sensors and Actuators Reports 4.
Chen, Y.Z., Li, Z.L., Xue, D.Y., Qi, L.M., 1987. Anal. Chem. 59, 744–748.
Chen, F., D'Auria, J.C., Tholl, D., Ross, J.R., Gershenzon, J., Noel, J.P., Pichersky, E., 2003. Plant J. 36, 577–588.
Chen, L., Wang, X., Lu, W., Wu, X., Li, J., 2016. Chem. Soc. Rev. 45, 2137–2211.
Chmela, O., Sadilek, J., Domenech-Gil, G., Sama, J., Somer, J., Mohan, R., Romano-Rodriguez, A., Hubalek, J., Vallejos, S., 2018. Nanoscale 10, 9087–9096.
Cho, S.H., Suh, J.M., Eom, T.H., Kim, T., Jang, H.W., 2020. Electronic Materials Letters, pp. 1–17.
Conti, S., Martinez-Domingo, C., Lay, M., Teres, L., Vilaseca, F., Ramon, E., 2020. *Advanced Materials Technologies* 5.
Crisp, P.A., Ganguly, D., Eichten, S.R., Borevitz, J.O., Pogson, B.J., 2016. Sci. Adv. 2.
De Fonseca, B., Rossignol, J., Stuerga, D., Pribetich, P., 2015. Urban Clim. 14, 502–515.
De Lacy Costello, B., Evans, P., Ewen, R., Gunson, H., Jones, P.R., Ratcliffe, N.M., Spencer-Phillips, P.T., 2001. Plant Pathol. 50, 489–496.
Deng, C., Zhang, X., Zhu, W., Qian, J., 2004a. Anal. Bioanal. Chem. 378, 518–522.
Deng, C.H., Zhang, X.M., Zhu, W.M., Qian, J., 2004b. Chromatographia 59, 263–268.
Deng, C.H., Qian, J., Zhu, W.M., Yang, X.F., Zhang, X.M., 2005. J. Separ. Sci. 28, 1137–1142.
Dicke, M., Baldwin, I.T., 2010. Trends Plant Sci. 15, 167–175.
Durrant, W.E., Dong, X., 2004. Annu. Rev. Phytopathol. 42, 185–209.
Fang, Y., Ramasamy, R.P., 2015. Biosensors 5, 537–561.
Fang, Y., Bullock, H., Lee, S.A., Sekar, N., Eiteman, M.A., Whitman, W.B., Ramasamy, R. P., 2016a. Biosens. Bioelectron. 85, 603–610.
Fang, Y., Umasankar, Y., Ramasamy, R.P., 2016b. Biosens. Bioelectron. 81, 39–45.
Fang, Y., Zhou, Y., Ramasamy, R.P., 2018. J. Electrochem. Soc. 165, B358.
FAO, F., 2017. Annual Report.
Garlando, U., Bar-On, L., Avni, A., Shacham-Diamand, Y., Demarchi, D., 2020. In: 2020 IEEE Sensors. IEEE.
Ge, L.P., Ye, X., Yu, Z.P., Chen, B., Liu, C.J., Guo, H., Zhang, S.Y., Sassa, F., Hayashi, K., 2022. *Npj Flex Electron* 6.
Grundler, P., Janata, J., 2008. Phys. Today 61, 53.
Hamilton, S., Hepher, M., Sommerville, J., 2005. Sensor. Actuator. B Chem. 107, 424–432.
Hilker, M., Schwachtje, J., Baier, M., Balazadeh, S., Baurle, I., Geiselhardt, S., Hincha, D. K., Kunze, R., Mueller-Roeber, B., Rillig, M.G., Rolff, J., Romeis, R., Schmulling, T., Steppuhn, A., van Dongen, J., Whitcomb, S.J., Wurst, S., Zuther, E., Kopka, J., 2016. Biol. Rev. 91, 1118–1133.
Hu, W., Wan, L., Jian, Y., Ren, C., Jin, K., Su, X., Bai, X., Haick, H., Yao, M., Wu, W., 2019. Adv. Mater. Technol. 4, 1800488.
Huang, J., Cardoza, Y.J., Schmelz, E.A., Raina, R., Engelberth, J., Tumlinson, J.H., 2003. Planta 217, 767–775.
Huang, Z.-h., Wang, Z.-l., Shi, B.-l., Wei, D., Chen, J.-x., Wang, S.-l., Gao, B.-j., 2015. Int. J. Anal. Chem.2015, 698630.
Ivaskovic, P., Ainseba, B.E., Nicolas, Y., Toupance, T., Tardy, P., Thiéry, D., 2021. ACS Sens. 6, 3824–3840.
James, T., Collins, S., Amlot, R., Marczylo, T., 2019. J. Chromatogr. B 1109, 84–89.
Janata, J.í., 2009. Conductometric sensors. In: Principles of Chemical Sensors. Springer, pp. 241–266.
Jansen, R.M., Hofstee, J.W., Wildt, J., Verstappen, F.W., Bouwmeester, H., van Henten, E.J., 2009. Plant Signal. Behav. 4, 824–829.
Jansen, R., Wildt, J., Kappers, I., Bouwmeester, H., Hofstee, J., Van Henten, E., 2011. Annu. Rev. Phytopathol. 49, 157–174.

Kakoty, P., Bhuyan, M., 2018. In: 2018 IEEE Electron Devices Kolkata Conference (EDKCON). IEEE.
Kanagasabapathy, M., Umasankar, Y., Bapu, G.R., 2014. Anal. Bioanal. Electrochem 6, 745–762.
Kanagasabapathy, M., Bapu, G.N.K.R., Umasankar, Y., Gnanamuthu, R.M., 2015. J. Electroanal. Chem. 754, 57–64.
Koo, Y.J., Kim, M.A., Kim, E.H., Song, J.T., Jung, C., Moon, J.K., Kim, J.H., Seo, H.S., Song, S.I., Kim, J.K., Lee, J.S., Cheong, J.J., Do Choi, Y., 2007. Plant Mol. Biol. 64, 1–15.
Krzek, J., Czekaj, J., Rzeszutko, W., 2003. Acta Poloniae Pharmaceutica. Drug Research 60.
Kumar, P., Kim, K.-H., Mehta, P.K., Ge, L., Lisak, G., 2019. Crit. Rev. Environ. Sci. Technol. 49, 2016–2048.
Lau, H., Liu, S.Q., Xu, Y.Q., Lassabliere, B., Sun, J., Yu, B., 2018. LWT (Lebensm.-Wiss. & Technol.) 94, 178–189.
Li, D.-W., Zhai, W.-L., Li, Y.-T., Long, Y.-T., 2014. Microchim. Acta 181, 23–43.
Li, Y., Li, Q., Wang, Y., Oh, J., Jin, S., Park, Y., Zhou, T., Zhao, B., Ruan, W., Jung, Y.M., 2018. Spectrochim. Acta Mol. Biomol. Spectrosc. 195, 172–175.
Li, Z., Paul, R., Ba Tis, T., Saville, A.C., Hansel, J.C., Yu, T., Ristaino, J.B., Wei, Q., 2019a. Nature plants 5, 856–866.
Li, J.D., Liu, X.J., Liang, X., Zhang, M.M., Han, L., Song, J.Y., 2019b. Sci. Rep. 9, 7.
Li, Z., Paul, R., Tis, T.B., Saville, A.C., Hansel, J.C., Yu, T., Ristaino, J.B., Wei, Q., 2019c. Nature plants 5, 856–866.
Li, F., Zheng, Y., Hua, C., Jian, J., 2019d. Front. Mater. 6, 101.
Li, Z., Zhao, L., Xie, F., Yang, C., Jayamanne, V.S., Tan, H., Jiang, X., Yang, H., 2021. J. Food Process. Preserv. 45, e15047.
Liu, B., Zhuang, J., Wei, G., 2020. Environ. Sci: Nano 7, 2195–2213.
Loreto, F., Schnitzler, J.P., 2010. Trends Plant Sci. 15, 154–166.
Madufor, N., Perold, W., Opara, U., 2017. In: VII International Conference on Managing Quality in Chains (MQUIC2017) and II International Symposium on Ornamentals in 1201.
Magagna, F., Cordero, C., Cagliero, C., Liberto, E., Rubiolo, P., Sgorbini, B., Bicchi, C., 2017. Food Chem. 225, 276–287.
Mahlein, A.-K., 2016. Plant Dis. 100, 241–251.
Matar, H., Guerreiro, A., Piletsky, S.A., Price, S.C., Chilcott, R.P., 2016. Cutan. Ocul. Toxicol. 35, 137–144.
Mauch-Mani, B., Baccelli, I., Luna, E., Flors, V., 2017. Annu. Rev. Plant Biol. 68, 485–512.
Mazurek, S., Szostak, R., 2016. Vib. Spectrosc. 83, 1–7.
Mishina, T.E., Zeier, J., 2007. Plant J. 50, 500–513.
Murugathas, T., Hamiaux, C., Colbert, D., Kralicek, A.V., Plank, N.O., Carraher, C., 2020. ACS Applied Electronic Materials 2, 3610–3617.
Nagraj, N., Slocik, J.M., Phillips, D.M., Kelley-Loughnane, N., Naik, R.R., Potyrailo, R.A., 2013. Analyst 138, 4334–4339.
Nguyen, H.H., Lee, S.H., Lee, U.J., Fermin, C.D., Kim, M., 2019. Materials 12, 121.
Oprea, A., Weimar, U., 2020. Analytical and Bioanalytical Chemistry, pp. 1–70.
Park, S.-W., Kaimoyo, E., Kumar, D., Mosher, S., Klessig, D.F., 2007. Science 318, 113–116.
Park, J., Thomasson, J.A., Fernando, S., Lee, K.-M., Herrman, T.J., 2019. Nanomaterials 9, 1621.
Park, J., Thomasson, J.A., Lee, K.-M., Suh, C.P.C., Perez, J.L., Herrman, T.J., 2020a. Anal. Methods 12, 1595–1605.
Park, J., Thomasson, J.A., Gale, C.C., Sword, G.A., Lee, K.-M., Herrman, T.J., Suh, C.P.C., 2020b. ACS Omega 5, 2779–2790.
Parker, D., Martinez, C., Stanley, C., Simmons, J., McIntyre, I.M., 2004. J. Anal. Toxicol. 28, 214–216.
Patel, S.V., Hobson, S.T., Cemalovic, S., Mlsna, T.E., 2008. Talanta 76, 872–877.
Pavey, K.D., FitzGerald, N.J., Nielsen, D.J., 2012. Anal. Methods 4, 2224–2227.
Pilot, R., Signorini, R., Fabris, L., 2018. In: Deepak, F.L. (Ed.), Metal Nanoparticles and Clusters: Advances in Synthesis, Properties and Applications. Springer International Publishing, Cham, pp. 89–164.
Potyrailo, R.A., 2016. Chem. Rev. 116, 11877–11923.
Rosser, K., Pavey, K., FitzGerald, N., Fatiaki, A., Neumann, D., Carr, D., Hanlon, B., Chahl, J., 2015. Rem. Sens. 7, 16865–16882.
Rowen, E., Gutensohn, M., Dudareva, N., Kaplan, I., 2017. J. Chem. Ecol. 43, 573–585.
Saiz-Rubio, V., Rovira-Más, F., 2020. Agronomy 10, 207.
Sedlackova, E., Bytesnikova, Z., Birgusova, E., Svec, P., Ashrafi, A.M., Estrela, P., Richtera, L., 2020. Materials 13.
Setka, M., Bahos, F.A., Matatagui, D., Potocek, M., Kral, Z., Drbohlavova, J., Gracia, I., Vallejos, S., 2020. Sensor Actuat B-Chem 304.
Shabir, G.A., Bradshaw, T.K., 2011. Turk J Pharm Sci 8, 117–126.
Sharma, P., Tudu, B., Bhuyan, L.P., Tamuly, P., Bhattacharyya, N., Bandyopadhyay, R., 2016. IEEE Sensor. J. 16, 5160–5166.
Shulaev, V., Silverman, P., Raskin, I., 1997. Nature 385, 718–721.
Silvester, D.S., 2011. Analyst 136, 4871–4882.
Singewar, K., Fladung, M., Robischon, M., 2021. Trees (Berl.) 35, 1755–1769.
Song, C., Guo, S., Jin, S., Chen, L., Jung, Y.M., 2020. Chemosensors 8, 118.
Stevens, S.G.E., Warren, B., 1964. J. Pharm. Pharmacol. 16, 32T–34T.
Tang, X., Raskin, J.-P., Lahem, D., Krumpmann, A., Decroly, A., Debliquy, M., 2017. Sensors 17, 675.
Tholl, D., Hossain, O., Weinhold, A., Rose, U.S.R., Wei, Q.S., 2021. Plant J. 106, 314–325.
Tomić, M., Šetka, M., Vojkůvka, L., Vallejos, S., 2021. Nanomaterials 11, 552.
Umasankar, Y., Ramasamy, R.P., 2013. Analyst 138, 6623–6631.
Vallejos, S., Gracia, I., Bravo, J., Figueras, E., Hubalek, J., Cane, C., 2015. Talanta 139, 27–34.
Vallejos, S., Gracia, I., Chmela, O., Figueras, E., Hubalek, J., Cane, C., 2016. Sensor Actuat B-Chem 235, 525–534.
Weber, J.H., 1977. Synthesis and Reactivity in Inorganic and Metal-Organic Chemistry, vol. 7, pp. 243–252.
Yang, C., 2020. Engineering 6, 528–532.
Yi, J., Xianyu, Y., 2022. Adv. Funct. Mater. 32, 2113012.
Zhang, Y., Liu, Q., Zhang, J., Zhu, Q., Zhu, Z., 2014. J. Mater. Chem. C 2, 10067–10072.
Zhang, Y., Zhang, J., Liu, Q., 2017. Sensors 17, 1567.
Zhang, W., Wang, R., Luo, F., Wang, P., Lin, Z., 2020. Chin. Chem. Lett. 31, 589–600.
Zhu, Q., Zhang, Y., Zhang, J., Zhu, Z., Liu, Q., 2015. Sensor. Actuator. B Chem. 207, 398–403.